Domain of metamers exciting intrinsically photosensitive retinal ganglion cells (ipRGCs) and rods

Françoise Viénot, Hans Brettel, Tuong-Vi Dang, Jean Le Rohellec

Domain of metamers exciting intrinsically photosensitive retinal ganglion cells (ipRGCs) and rods

Françoise Viénot,[1,*] **Hans Brettel,**[2] **Tuong-Vi Dang,**[1,3] **and Jean Le Rohellec**[1]

[1]*Centre de Recherche sur la Conservation des Collections, Muséum National d'Histoire Naturelle,
36 rue Geoffroy Saint-Hilaire, F-75005 Paris, France*
[2]*CNRS LTCI, Telecom ParisTech, 46 rue Barrault, F-75013 Paris, France*
[3]*Licence ATI, Université de Caen Basse-Normandie, Boulevard Maréchal Juin, 14032 Caen Cedex 5, France*
*Corresponding author: vienot@mnhn.fr

Any stimulus can be described as composed of two components—a fundamental color stimulus that controls the three cone responses and a metameric black that has no effect on cones but can drive photoreceptors other than cones [e.g., rods and melanopsin expressing retinal ganglion cells (ipRGCs)]. The Cohen and Kappauf [Am. J. Psychol. **95**, 537 (1982)] method is extended to calculate the black metamer basis for a limited set of band spectra. Using seven colored LEDs, the method is exploited to produce real metamer illuminations that stimulate in parallel melanopsin expressing ipRGCs and rods, at most or at least. We have verified that the pupil diameter increases when the ipRGC and rod excitation is at a minimum. For 14 observers, the average relative increase is 12%.   © 2012 Optical Society of America

OCIS codes: 330.1715, 330.1720, 330.5310, 330.4595, 230.3670.

1. INTRODUCTION

Whereas the main input to visual images comprises cones and rods, a small subset of retinal ganglion cells (ipRGCs) in mammals express the photopigment melanopsin. They depolarize to light, even when all synaptic inputs from rods and cones are blocked. They are intrinsically photosensitive.

Initially described in rodents [1,2], the ipRGCs were shown in primates [3,4], where they project to the lateral geniculate nucleus (LGN) and to brain areas involved in nonimage-forming visual functions. They project primarily to the olivary pretectal nucleus (OPN), which drives the pupillary light reflex (PLR), and to the suprachiasmatic nucleus of the hypothalamus (SCN), which controls circadian rhythms [5]). In the macaque-monkey retina, there are about 3000 ipRGCs, constituting 0.2% of the total retinal ganglion cells (RGC) population. The ipRGC dendrites, also photosensitive, form an extensive and overlapping mesh that covers the entire retina except for the fovea [3].

Thus, five photoreceptors are present in the retina: *L*-cones, *M*-cones, *S*-cones and rods, responsible for image vision, and the melanopsin expressing ipRGCs. With respect to the full visual response, comprising image processing and visual nonimaging response, the stimulus is defined as a five-dimensional vector.

A. ipRGCs, Rods, and Cones

In the macaque monkey, in addition to being photosensitive to direct stimulation by light, ipRGCs are strongly activated by rods and cones, via synaptic complex networking. Thus, they integrate and convey inner and outer retinal signals to non-image-forming visual areas [3,5,6]. The synaptic input to ipRGCs is broadly similar to that of a mouse, with the exception that both ON and OFF responses are prominent, the latter originating from *S*-cones [3] (see the review in [5]).

In primates, as in rodents, subclasses have been distinguished based on morphology and absolute photosensitivity. These ipRGC subtypes also differ with respect to their retinal circuitry. In the primate retina, they appear to be principally monostratified, with subtype M1 stratifying in the OFF sublamina of the inner plexiform layer and subtype M2 stratifying in the ON sublamina close to the ganglion cell layer [3,4]. Paradoxically, OFF-stratifying M1 cells receive input from the ON pathway within the OFF sublamina of the inner plexiform layer. Using pharmacological tools and single-cell recordings of synaptic responses in wild-type and melanopsin-null mice, Schmidt and Kofuji found that the ON pathway forms the primary excitatory synaptic input to both M1 and M2 cells [7].

In response to an increment of light, rodents' and macaques' ipRGCs exhibit a transient firing peak that decays to a steady plateau that continues well past stimulus cessation [1,2,3,6,8]. The relaxation that follows the transient peak indicates light adaptation, and the progressive recovery in darkness indicates dark adaptation [6]. Outer retinal photoreceptors also contribute to sustained firing during long duration light stimuli [6].

The spectral efficiency of melanopsin photoreception in both rodents and humans has been estimated by comparing sensitivity to several near monochromatic stimuli as a function of wavelength. The resultant action spectrum is well-fitted by a vitamin A1 visual pigment nomogram, and there is a general agreement for a peak spectral sensitivity about 480–482 nm [1,3,9,10,11].

Dacey [3] recorded the response of a giant cell, likely an ipRGC, to a 470 nm light step as a function of retinal illuminance for three stimulus conditions. Under pharmacological blockade of all synaptic transmission, the sustained depolarization of the isolated ipRGC was measured at 470 nm above 11 log quanta cm^{-2} s^{-1}, indicating the melanopsin sensitivity

range. Without pharmacological blockade of the cone input, it was possible to observe a summation of short-latency depolarizing cone response and slow rod response over most of the photopic range above 10 log quanta $cm^{-2} s^{-1}$. In the dark-adapted state, from as low as 6–7 log quanta $cm^{-2} s^{-1}$ up to 10 log quanta $cm^{-2} s^{-1}$, which is well below the threshold of the melanopsin photo response, the ipRGC cell maintains its response to light stimuli, indicating a pure rod response [6].

In ipRGCs, the melanopsin signal is more like a bistable invertebrate opsin signal than like a vertebrate rod-and-cone opsin signal [12,13,14,15]. Unlike rod-and-cone pigments, which are bleachable, in that the photoisomerized chromophore ultimately dissociates from the opsin and regenerates in the retinal pigment epithelium (RPE), melanopsin cells may have a RPE-independent photoregeneration system, with a conversion from melanopsin into metamelanopsin at about 480 nm and the converse at a higher wavelength [13]. Nevertheless, not all data support this model [16,17].

B. Pupil Light Response
When the human eye is exposed to a light increment, the pupil constricts transiently and then recovers toward a steady-state diameter [11,17,18]. See the review in [11].

The main arguments in favor of the control of the pupillary response by melanopsin were described by Gamlin et al. [10], who reported that, in the behaving macaque, following pharmacological blockade of rod-and-cone signals, significant pupil response persists during continuous light. Following light offset, there is a transient pupil dilation followed by a sustained constriction. In the macaque, the sustained pupillary responses are elicited by light of 493 nm but not of 613 nm. The spectral sensitivity data derived during pharmacological blockade as well as from the poststimulus sustained pupillary response under normal conditions closely matches the spectral sensitivity of melanopsin, which is maximally sensitive to 482–483 nm light.

These results demonstrate in macaques that the melanopsin signal contributes significantly to sustained light-evoked pupillary responses; they also show in primates that the melanopsin signal is primarily responsible for the sustained pupilloconstriction that occurs following light offset.

The human pupil light response exhibits complex kinetics that reveal the contributions of rods, cones, and melanopsin expressing ipRGCs. McDougal and Gamlin [17] examined the relative receptor contribution to the pupil light reflex in response to monochromatic light stimuli (9.5–15 log quanta $cm^{-2} s^{-1}$) presented for approximately 4, 12, 34, or 110 s. In response to steady-state light steps, within 10 s of light onset, cones contribute to the transient portion on the pupil light reflex but minimally to the maintenance of steady-state pupillary diameter at both low and high photopic irradiances. The melanopsin photoresponse of ipRGCs not only contributes to pupillary constriction at high irradiances but also acts to maintain pupillary diameter in steady-state photopic lighting conditions. Rod contribution to the PLR also adapts over time but reaches a steady state at which rods contribute to steady-state pupillary constriction at irradiances that are below threshold for the melanopsin photoresponse [17].

After the cessation of a bright visual stimulus, the pupil dilates and stabilizes at a diameter value less than prior to stimulus onset. This postillumination pupil reflex has been observed following a photopic 10 s, wide-field, 470 nm light stimulus but not a 623 nm stimulus, which is consistent with the melanopsin-mediated response [19].

Comparisons between human responses to short- and long-wavelength stimuli reveal pupil contraction differences [20]. In humans, the peak of melanopsin stimulation and pupillary reflex *in vivo*, close to 480 nm, seems to be [13,21,22] identical to the light response of isolated ganglion cells. Gamlin et al. [10] also showed that the poststimulus sustained pupillary response in humans has a spectral sensitivity close to the vitamin A1 pigment nomogram with peak sensitivity at 482 nm, which provides evidence for the existence of a functional, melanopsin-driven inner retinal pathway in humans.

C. Metamers, Black Metamers, Pupil Response
Metamers are visual stimuli with different spectra that look identical to the observer. Cone metamers initiate the same excitation in the three families of cones. The difference of spectral content may be captured by any other photopigment. A few experiments have already been conducted to correlate the pupil aperture with the spectral content of illumination in primates and humans [3,10,11,13,17,23,24].

In this paper, we examine to what extent cone metamers address rods and ipRGCs differently. We develop a method dedicated to the excitation of any receptors besides cones. In the first part of the paper, we will consider the theory of metamers, precisely the role of black metamers not involving color vision. Because, as it will be explained in the next section, black metamers have no effect on cones but may have an effect on receptors with different spectral sensitivity such as rods and ipRGCs, we investigate the feasibility of a method based on black metamers to independently address receptors of known spectral sensitivity. In the second part of the paper, we will describe an experiment where we have exploited the theory of metamers to produce real illuminations using light-emitting diodes (LED) to optimize the production of visual but nonimaging responses of observers.

2. THEORETICAL APPROACH: BLACK METAMERS

A. Wyszecki Proposal
The theoretical approach consists of examining the efficiency of black metamers to elicit a melanopsin signal in ipRGCs and a rod signal. Considering that any stimulus can be described as composed of two components—a fundamental color stimulus and a metameric black [25,26]—a black metamer basis is built, and the corresponding ipRGC and rod signals are calculated.

As the computational procedures for the separation of any stimulus N into its fundamental component N^* and its metameric black component B,

$$N = N^* + B,$$

are given in full detail by Cohen and Kappauf [26], we here refer to their presentation.

By uniformly sampling the spectrum of a visual stimulus into k equal wavelength intervals, any stimulus can be represented by a $(k \times 1)$-dimensional vector N of its radiometric

power distribution.

$$N = [N_{\lambda 1} \quad N_{\lambda 2}...N_{\lambda k}]'.$$

Using a $k \times 3$ matrix A representing an equally sampled version of the observer's color-matching functions, tristimulus values T are obtained as a (3×1)-dimensional vector by the matrix product

$$T = A'N. \tag{1}$$

For example, for the case of the CIE 1964 system, A' is the transpose of

$$A = [X_{10} \quad Y_{10} \quad Z_{10}],$$

where each of X_{10}, Y_{10}, and Z_{10} are $(k \times 1)$-dimensional vectors representing the 10-deg color-matching functions sampled at k equal wavelength intervals.

Black metamers B are such theoretical spectral functions for which all three tristimulus values are zero:

$$A'B = [0 \quad 0 \quad 0]'.$$

Although all possible functions B do not produce a response in the cones, they generally will produce a response in ipRGCs and rods.

B. Extension of the Cohen and Kappauf Procedure to Multi-LED Illumination

1. Extension of the Cohen and Kappauf Procedure to Any Spectral Basis

The procedure that accomplishes the decomposition of any spectral energy distribution into its two parts, as described by Cohen and Kappauf [26], can be extended to any color-stimulus function specified in a spectroradiometric basis. Cohen and Kappauf have presented a precise demonstration for a spectrum consisting of only six spectral lines.

2. Application of the Procedure to Seven-LED Illumination

Here, our objective is to investigate the domain of white metamers produced by the full range of seven-color LED mixtures illuminating a light booth and examine their effect on visual responses besides color. Our white metamers are light stimuli of different spectral composition that all produce, in the three types of retinal cones, the same excitations as a "white" stimulus of 5350 K color temperature. We extend the Cohen and Kappauf procedure to a radiometric space of seven band spectra. Practically, the seven band spectra are produced by seven-color LEDs, driven at maximum intensity (Fig. 1).

The primary calculation consists in building the 7×3 matrix A_7 that includes the tristimulus values of individual color LEDs driven at maximum intensity. Peak wavelengths of the seven LEDs, named royal blue, blue, cyan, green, amber, red and far red LEDs, are located at $\lambda_{\text{peak}} = 447, 472, 502, 523, 594, 637$, and 656 nm. Here, actual full spectroradiometric data are used for building a spectral basis of seven components.

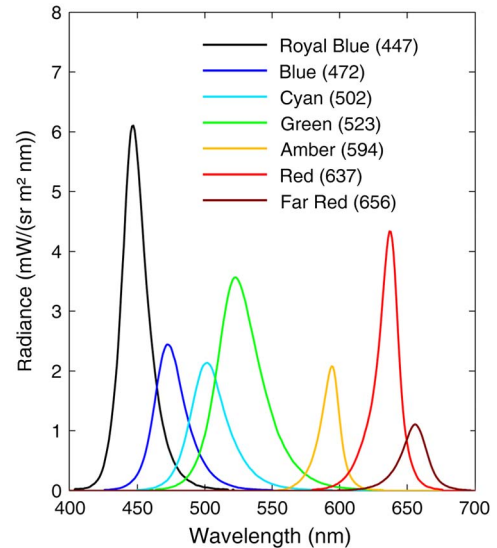By representing each of the seven LEDs by a $k \times 1$ vector P_i of its spectral power distribution

Fig. 1.   (Color online) Spectral power distribution of the light emitted by the color LEDs. Peak wavelength as indicated in the inset, in nm. LED spectra ranging from short to long wavelengths correspond to labels listed top to bottom.

$$P_i = [P_{i,\lambda 1} \quad P_{i,\lambda 2} \quad P_{i,\lambda 3}...P_{i,\lambda k}]' \qquad i = 1,...,7,$$

any possible light stimulus N obtained by additive mixture from these LEDs can be written as

$$N = L_1 P_1 + L_2 P_2 + L_3 P_3 + L_4 P_4 + L_5 P_5 + L_6 P_6 + L_7 P_7. \tag{2}$$

N is a $k \times 1$ vector, and $L_1,...,L_7$ are the relative contributions of each LED.

With the 7×1 vector $L = [L_1 \quad L_2 \quad L_3 \quad L_4 \quad L_5 \quad L_6 \quad L_7]'$ and the $k \times 7$ matrix $P = [P_1 \quad P_2 \quad P_3 \quad P_4 \quad P_5 \quad P_6 \quad P_7]]$, Eq. (2) writes in matrix notation

$$N = PL. \tag{3}$$

Since the matrix A of the observer's color-matching functions and the matrix P of the spectral power distributions of the LEDs are constant with respect to our experiments, we can use a prebuilt 7×3 matrix A_7 instead of the full $k \times 3$ matrix A introduced by Cohen and Kappauf [7].

$$A_7 = P'A. \tag{4}$$

The tristimulus values of A_7 that result from the scalar product of the LED spectral radiance and the color-matching functions could be derived in any colorimetric basis $(X \quad Y \quad Z)$ or $(L \quad M \quad S)$. Here we choose the $(X_{10} \quad Y_{10} \quad Z_{10})$ colorimetric basis to prepare future experimental validation on a large field of view. Then the 7×7 matrix R_7 is calculated as

$$R_7 = A_7(A_7' \quad A_7)A_7'. \tag{5}$$

R_7 is a symmetric matrix. It is the orthogonal projector that projects any light stimulus obtained by additive mixture from the seven LEDs in the color space.

The relative contributions of each of the seven LEDs to produce a light stimulus N are, according to Eqs. (2) and (3), the elements $L_1, L_2,...,L_7$ of the 7×1 vector L, and the projector

R_7 applies as

$$L^* = R_7 L. \tag{6}$$

The elements of the 7×1 vector L^* are the relative contributions of each of the seven LEDs to produce a light stimulus N^*, which is fully embedded in the fundamental color-stimulus space. Finally, the $(k \times 1)$-dimensional spectral power distribution of N^* is obtained as

$$N^* = PL^*. \tag{7}$$

The same formal procedure as given by Eqs. (6) and (7) can be used for the black metamers. But instead of R_7, we need a corresponding 7×7 matrix B_7, which represents the set of black metamers for our seven LEDs. B_7 is obtained by subtracting R_7 from the 7×7 identity matrix I_7.

$$B_7 = I_7 - R_7. \tag{8}$$

The rows or columns of the symmetric 7×7 matrix B_7 contain the relative contributions of each of the seven LEDs to produce seven different black metamers; these values are shown as bar charts in Fig. 2. The resulting spectral power distributions of the black metamers, shown in Fig. 3, are obtained by using these LED contributions as L in Eq. (3).

Given a target white W at 5350 K, typical of a commercial phosphor converted white LED, we easily calculate which unique mixture of three LEDs, say blue, green, and red LEDs, matches the target. The result provides us with a seminal metamer N, i.e., the one that yields the fundamental metamer N^* of the target white. The left panel of Fig. 4 shows the seven-color LED composition of the white metamer corresponding to the target white W.

C. Optimizing the ipRGC and Rod Excitations. Numerical Predictions

1. About the Difficulty of Separating ipRGC and Rod Excitation

The effect of any illumination can be separated into the effect of its mixture components. The fundamental metamer controls the three cone responses. The black metamer component has no effect on cones. Its tristimulus values are (0, 0, 0). Conversely, it has an effect on any receptor of which the spectral sensitivity is different from the cone spectral sensitivity. In other words, any experimental procedure that takes into account "black metamers" only is silent for cones. Therefore, the black metamer component drives the rod and the
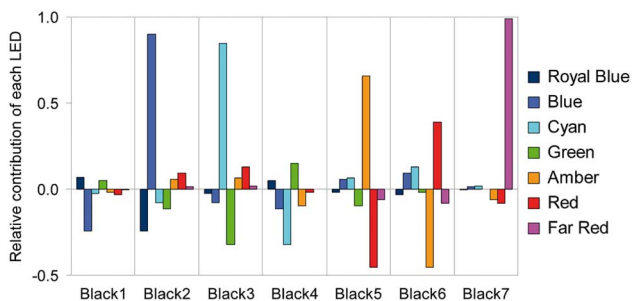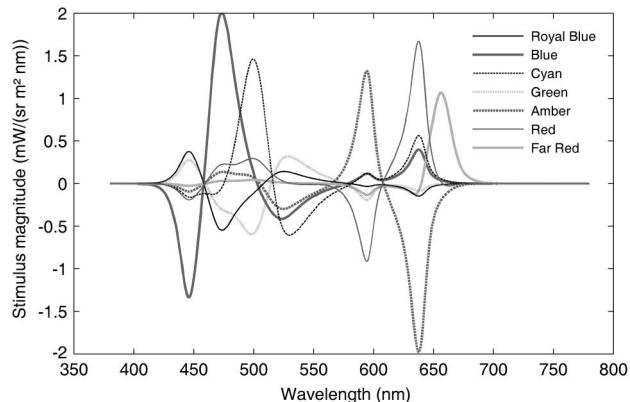
Fig. 3.   Relative color-stimulus function of each black metamer.

ipRGC responses. The total effect of the light is the sum of the fundamental and the black metamers effects.

Theoretically, receptor signals can be separated as soon as their action spectra are independent and different and as an equal or higher number of primary stimuli are available.

The action spectra for *S*-cones, *M*-cones, and *L*-cones are given by the cone fundamentals [27,28]. The action spectrum for rods is given by the spectral luminous efficiency function of the CIE standard photometric observer for scotopic vision $V'(\lambda)$ [29]. We have hypothesized that the spectral template of the melanopsin photopigment is the same as the template of rod-and-cone rhodopsin. Thus, starting with the low density absorbance spectra of the visual pigments proposed by Stockman and Sharpe [27], we applied a shift of the template along the frequency axis, so as to position the peak at 482 nm [3,11,24]. Then, we reconstructed the action spectrum of the ipRGCs at the corneal plane. Because dendrites and cell bodies of ipRGCs are thin and the density of melanopsin is small [30] compared with the cone external segment, we could assume a small optical density (equal to 0.1) for the photopigment. No correction was introduced for macular pigmentation, which absorbs light at the back of the ganglion cell layer. The lens spectral absorbance proposed by Stockman

Fig. 2.   (Color online) Bar chart of each black metamer expressed in terms of seven-color LED components.
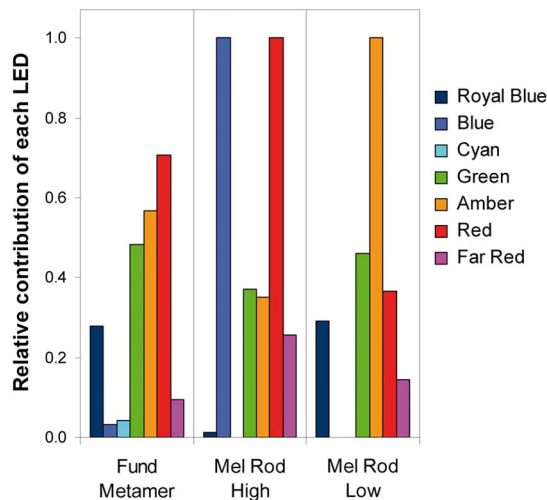
Fig. 4.   (Color online) Bar graph of the multicolour LED illuminations that would produce the fundamental metamer of the 5350 K white and that excite melanopsin and rods at most and at least, expressed in terms of seven-color LED components.

and Sharpe [27] could apply to our young observers. Thus, the stimulus that elicits the response of ipRGCs is proportional to the integral of the product of the spectral power distribution of the LED illumination and the action spectrum of ipRGCs. Our calculation implies additivity of the melanopsin phototransduction, a property that has been assessed in the circadian response of rodents [31,32].

Al Enezi et al. [31] have shown that pupillomotor and circadian responses of mice relying solely on melanopsin for their photosensitivity can indeed be accurately predicted using a similar methodology. Their "melanopic" sensitivity relevant for melanopsin photoreception is based on the 480 nm nomogram. They have also shown that measuring light in these terms reliably predicts the melanopsin response to light of divergent spectral composition much more reliably than photometric quantities. Their spectral sensitivity function $V^z(\lambda)$, available online, is slightly shifted with respect to ours.

Finally, although separating ipRGC and rod excitation is theoretically possible, it is difficult to achieve on a purely spectral basis because their spectral sensitivities largely overlap. This can be verified by plotting the rod stimulus value versus the ipRGC stimulus value of the black metamers (Fig. 5). In Fig. 5, rod and ipRGC excitations have been calculated using an action spectrum normalized to unity at peak wavelength and multiplied by 683.

2. Controlling Seven LEDs Intensity

Once the fundamental metamer and the set of seven black metamers being calculated were determined, we used the generalized reduced gradient (GRG2) algorithm proposed by the Microsoft Excel solver to look for the seven-LED component solution, which either maximizes or minimizes the rod and ipRGC excitations. The only restriction imposed to the solution concerns the feasibility of the illumination; all LEDs should be addressed between 0 and 1 (Fig. 4, middle and right panels).

Figure 6 shows the actual spectral power distribution of the fundamental metamer, the "Mel Rod High" and the "Mel Rod Low," which are all cone metamers.

Results of the predictions are given in Table 1. As mentioned earlier, calculations [33] were made in the $(X_{10} \quad Y_{10} \quad Z_{10})$ colorimetric basis in order to stabilize the solver solution. Lines X_{10}, Y_{10}, and Z_{10} show that the funda-
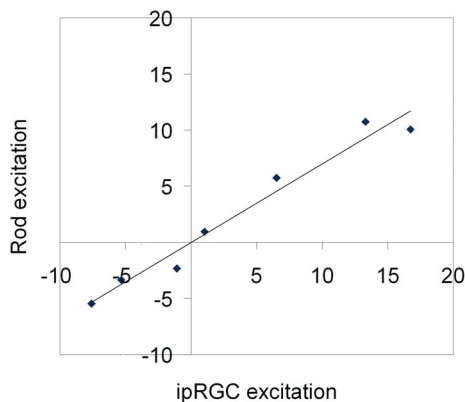

Fig. 5. (Color online) Rod excitation versus ipRGC excitation achieved by every black metamer. Arbitrary units: rod and ipRGC excitations have been calculated using an action spectrum normalized to unity at peak wavelength and multiplied by 683.
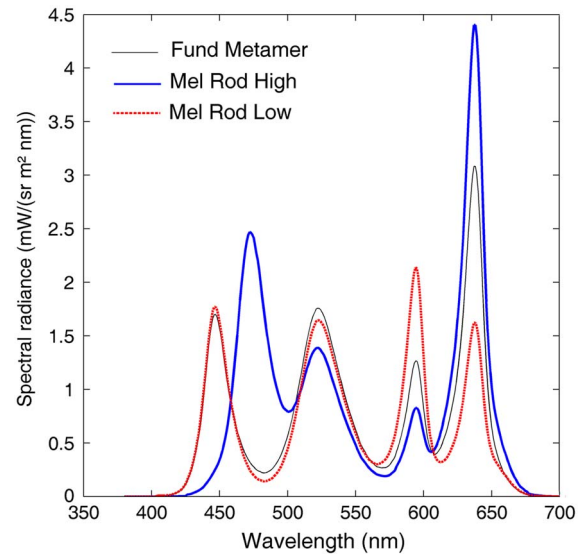

Fig. 6. (Color online) Fundamental metamer and multicolor LED illuminations that excite melanopsin and rods at most (thick blue line) and at least (broken orange line), respectively. The thin black line represents the fundamental metamer. Measurements were taken at the wall of the light booth facing the observer.

mental metamer and the Mel Rod High and the Mel Rod Low illuminations are true metamers. The five following lines give the results in arbitrary units. The amounts of receptor excitation were calculated using receptor sensitivity functions that culminate at one [27,28] and multiplying the scalar product of the stimulus and the sensitivity by 683. This choice of arbitrary units allows us to estimate easily the response of each type of receptor. These values have served to graphically represent the effect of the Mel Rod High and the Mel Rod Low on the five types of receptors (Fig. 7). Calculation allows us to predict that we could produce a 1.53 contrast for ipRGCs and a 1.32 contrast for rods between the two illuminations (Table 2, third column), at the corneal entrance.

3. EXPERIMENTAL METHODS

The rationale of the experiment is to adjust the spectral power distribution of metamer white LED illuminations to excite rods and ipRGCs at most or at least. The white target color is that of a typical commercial white LED specified by its color temperature, and metamer illuminations are produced by adjusting the intensity of seven-color LEDs. The ipRGC response is not directly measured, but the sustained pupil response, which is assumed to be under rods' and ipRGCs' control at low photopic levels or under ipRGCs' control at photopic levels, is recorded, following a sudden change of illumination.

A. LED Calibration

Several white and color LED clusters were mounted on heat radiators and housed inside the ceiling of a light booth $(W \times H \times D = 1.0 \times 0.6 \times 0.5 \text{ m})$. We could modulate royal blue, blue, cyan, green, amber, red, far red LEDs (Fig. 1). Each family of LEDs was controlled by its own driver through a pulse width modulation (PWM) power supply. Heat radiators were dimensioned so as to avoid heating that could modify emission during the experiment. Several diffusers were included in the ceiling of the booth to mix the color beam of the LEDs. The walls and floor of the booth were painted white

Table 1. Prediction of the Receptor Excitations Corresponding to the Fundamental Metamer and Black Metamer Components of the Seven-Color LED Illuminations That Excite ipRGC and Rods at Most (Mel Rod High) or at Least (Mel Rod Low), in Arbitrary Units: All Excitations Calculated Using an Action Spectrum Normalized to Unity at Peak Wavelength and Multiplied by 683

	Fundamental metamer component	Mel Rod High black metamer component	Mel Rod High stimulus	Mel Rod Low black metamer component	Mel Rod Low stimulus
			Tristimulus values		
X_{10}	65.05	0.00	65.05	0.00	65.05
Y_{10}	66.66	0.00	66.66	0.00	66.66
Z_{10}	57.71	0.00	57.71	0.00	57.71
			Receptor excitations (Arbitrary units as explained in the caption)		
ipRGC	48.31	20.24	68.55	−3.61	44.70
Rod	55.75	13.14	68.89	−3.60	52.15
S-cone	27.56	−0.90	26.66	0.08	27.64
M-cone	58.06	0.20	58.26	0.01	58.07
L-cone	68.23	0.04	68.28	0.13	68.37

to ensure Ganzfeld-like illumination. A 5° aperture at the back of the light booth was open to position the camera behind the hole.

The full system was interfaced with a computer through a DMX512 control system. Each family of LEDs could be dimmed using proprietary software (©LedToLite) associated with the DMX control box. Each family of LEDs was addressed with a digital level from 0 to 255.

Prior to the experiment, each family of LEDs was calibrated individually. For a series of DMX values D_i, we measured the spectral power distribution of the light reflected at the wall of the light booth facing the observer and calculated the corresponding $X_{10,i}$, $Y_{10,i}$, and $Z_{10,I}$ degrees tristimulus values. A second-order polynomial regression line was fitted to each series of Y_{10} values.

Although the chromaticity of LED is known to vary with the input voltage, the chromaticity stability ($|\Delta x| < 0.0023$, $|\Delta y| < 0.0013$ for the amber LED, which is the least stable item) was judged sufficient to prepare the right experimental setup. Finally, the spectral power distribution of all illuminations was measured *in situ* using a JETI specbos 1211UV spectroradiometer aimed close to the hole open in the back wall of the light booth, facing the observer.
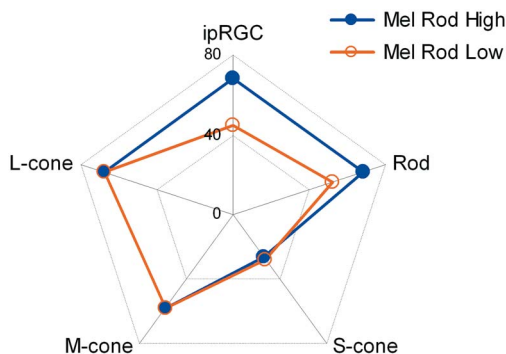

Fig. 7. (Color online) Prediction of receptor relative excitations obtained from the multicolor LED illuminations that excite melanopsin and rods at most (thick blue line) and at least (thick orange line), respectively. Arbitrary units: All receptor excitations have been calculated using an action spectrum normalized to unity at peak wavelength and multiplied by 683.

B. Illumination

Two illuminations were prepared, metameric to a white stimulus of 5350 K color temperature, named "Mel Rod High" and "Mel Rod Low," respectively, maximizing rod and ipRGC excitation and minimizing rod and ipRGC excitation, as calculated in the section "Controlling Seven LEDs Intensity." The planned scenario consisted in the succession of three two-minute sequences: "Mel Rod High"/"Mel Rod Low"/"Mel Rod High." Thus, examination of the pupil response under each illumination could be obtained following the alternate illumination.

For a technical reason, the far red color LED has been driven at a maximum intensity in the Mel Rod High experimental configuration, which has had a minor effect on ipRGC and rod excitations but has slightly increased the contrast of the long-wave sensitive (LWS) and middle-wave-sensitive (MWS) cone excitations. We have controlled the illumination, and we report in Table 2 the controlled values obtained at the end of the experiment. Parts "Tristimulus values" and "Receptor excitations" in Table 2 allow us to compare the real measurements with the predictions. The experimental values of ipRGC and rod contrast are equal to 1.66 and 1.44, respectively. Then comes the part giving the real photometric quantities, calculated using the measured spectral power distributions and the tabulated data of the CIE standard photometric observer or the CIE fundamentals.

The LWS and MWS cone excitation contributions sum to the luminance, using the $L:M = 1.98:1$ ratio [34]. The slight discrepancy between the 10° luminance value Y_{10} and the sum of contribution of the LWS and MWS cone excitation originates from the different choices of original colorimetric data between the CIE 1964 standard colorimetric observer and the CIE cone fundamentals.

In the last four lines of Table 2, we have converted the receptor excitations measured at the eye entrance to photometric quantities at the retinal image, for comparison with published studies where retinas are mounted and illuminated *in vitro*. Using the formula proposed by Le Grand [35]

$$E_p = 0.36 \int L_p(\lambda) S\tau(\lambda) \mathrm{d}\lambda$$

to obtain the total irradiance of the retinal image given by the white illumination, we converted the measured spectral

Table 2.   Predicted and Experimental Photometric Quantities and Receptor Excitation Values Corresponding to the "Mel Rod High" and "Mel Rod Low" Configurations: Retinal Irradiance Values Calculated Using the Average Diameter of the Observer Pupils

	Mel Rod High, predicted	Mel Rod Low, predicted	Max/Min ratio, predicted	Mel Rod High, experimental	Mel Rod Low, experimental	Max/Min ratio, experimental
Tristimulus values						
X_{10}	65.05	65.05		66.07	64.01	
Y_{10}	66.66	66.66	1	71.11	65.76	1.08
Z_{10}	57.71	57.71		59.21	59.49	
Receptor excitations (Arbitrary units as in Table 1)						
ipRGC	68.55	44.70	1.53	75.14	45.35	1.66
Rod	68.89	52.15	1.32	76.12	52.70	1.44
S-cone	26.66	27.64	0.96	27.30	28.50	0.96
M-cone	58.26	58.07	1.00	63.45	57.61	1.10
L-cone	68.28	68.37	1.00	72.28	67.31	1.07
Photometric quantities						
Luminance ($\mathrm{cd\,m^{-2}}$)				62.57	61.24	1.02
M-cone contribution to Y_{10}				23.86	22.07	1.08
L-cone contribution to Y_{10}				47.25	43.69	1.08
Scotopic luminance ($\mathrm{cd\,m^{-2}}$)				189.47	131.18	1.66
Photometric quantities converted at the retinal image						
Average pupil diameter of the observers (cm)				0.46	0.53	
Scotopic retinal level (Trolands)				3149	2894	1.088
Total irradiance of the retinal image (log quanta $\mathrm{cm^{-2}\,s^{-1}}$)				12.61	12.58	1.09
ipRGC-weighted irradiance of the retinal image (log quanta $\mathrm{cm^{-2}\,s^{-1}}$)				12.07	11.98	1.24
Rod-weighted irradiance of the retinal image (log quanta $\mathrm{cm^{-2}\,s^{-1}}$)				12.11	12.08	1.07

power distribution $L_e(\lambda)$ into spectral photon radiance $L_p(\lambda)$ expressed in quanta $\mathrm{cm^{-2}\,s^{-1}\,nm^{-1}}$, multiplied it by the spectral transmittance of the eye $\tau(\lambda)$ [36], summed the values over the visible spectrum, and entered the real average pupil diameter obtained from our experiments. When the surface S of the pupil is expressed in $\mathrm{cm^2}$ and the spectral photon radiance L_p is expressed in quanta $\mathrm{cm^{-2}\,sr^{-1}\,nm^{-1}\,s^{-1}}$, the photon irradiance E_p is expressed in quanta $\mathrm{cm^{-2}\,s^{-1}}$.

We calculated the rod-weighted irradiance replacing the spectral transmittance of the eye by the CIE standard photometric observer for scotopic vision $V'(\lambda)$. We performed similar calculations to obtain ipRGC-weighted irradiance replacing the spectral transmittance of the eye by the ipRGC action spectrum.

C. Observers

Fourteen volunteer observers, aged 20–35 years, with normal acuity and with normal color vision assessed by pseudoisochromatic plates or the panel D15 color vision test, took part in the experiment. They gave a written consent prior to the experiment.

The observer sat in front of the light booth and positioned his(her) head on a chin rest. He(she) viewed binocularly the whole interior of the light booth, covering 180° viewing angle. He(she) was instructed to keep his(her) eyes open and fixate a line of letters (angular height 12′) glued just above the hole for the camera in order to minimize accommodation-driven pupil fluctuations.

D. Photographs

As soon as the illumination scenario had started, photographs were taken every 5 seconds up to the end of the scenario. The first two-minute sequence, Mel Rod High, served to preadapt the observer to the following Mel Rod Low illumination. To evaluate the sustained response, although photographs were captured immediately after the substitution of one light to the other, only the last 12 shots of the two-minute sequence were processed, i.e., photographs acquired after one minute of illumination. Photographs were obtained with a Canon EOS 550D digital camera, computer controlled. As explained in the section "Illumination," the succession of sequences was planned to allow the Mel Rod Low as well as the Mel Rod High configurations to be examined after two minutes of the alternate configuration.

The right eye image, about 560×170 pixels, was manually extracted from the photograph. Then the iris contour and the pupil contour were automatically extracted after writing a MATLAB program including thresholding and aperture scripts and the analytical function of a circle. For every image, the program delivers the ratio of the pupil-to-iris diameter and displays the original image with two encrypted circles for visual control of the output.

4. EXPERIMENTAL RESULTS

A. Measurements

Following the metamer illumination substitution, the pupil aperture changes for about 15 seconds and then stabilizes.

Only images captured during the second minute of the two-minute illumination sequence were processed. A few photographs had to be rejected because the observer had closed his(her) eyes. Twelve measurements of the pupil aperture were averaged.

As an example, Fig. 8 shows the variation of pupil aperture of one observer (observer #1) during the full Mel Rod Low sequence that followed switching from Mel Rod High to Mel Rod Low illumination (Fig. 8, left panel). For this observer, the rapid dilation of the pupil was captured on the two first photographs; then the pupil seemed to slightly constrict before stabilizing. The graph also shows the results obtained during the converse full sequence Mel Rod High that followed switching from Mel Rod Low to Mel Rod High illumination (Fig. 8, right panel). The first three photographs captured the rapid constriction to a minimum, which is followed by a plateau. The pupil diameter is expressed relative to the iris diameter, as calculated from the counts of pixels along the two diameters.

To provide information about the reproducibility of the measurements, the graph also shows two lines that represent the corresponding pixel counts (in kilopixels) along the iris diameter. Besides slight variations from one photograph to the next, the iris diameter values are nearly equal over the Mel Rod High and Mel Rod Low illuminations.

Results of 14 observers are shown in Fig. 9 with individual standard deviations. All observers show a sustained constriction when the ipRGC and rod excitation is at a maximum. The paired Wilcoxon test shows a significant effect (at $p < 0.05$) for 12 of the 14 observers. As an average among the observers, the relative variation of the sustained pupil constriction is 0.12, as shown on the right of the figure.

Not all observers have the same pupil diameter. Because the original shot includes an image of the face together with the vertical side bars of the head restraint, we can recover the actual size of the pupil from converting the number of pixels in the image to a metric distance in mm. The average variation of 12% of the pupil diameter corresponds to a reduction of pupil diameter from 5.3 mm to 4.6 mm. Some observers spontaneously reported a brightness increase at the establishment of the Mel Rod High illumination.

5. DISCUSSION

A. Value of Adopting the Scheme of Black Metamers
As explained by the promoters of the black metamers theory [25,26], any spectral energy distribution consists, mathematically at least, of two component wavelength distributions: the fundamental metamer that contributes to the color specification of the stimulus, hence to the perceived color, and a black metamer component that elicits no cone response. Thus, black metamers open the way to a systematic investigation of the ipRGC and rod function.

Compared to the silent substitution paradigm [37], black metamers offer an opportunity to screen the whole domain of metamer stimuli that elicit any other response than the cones' response. Exploring the domain of black metamers is an efficient method to optimize the spectral power distribution that controls at best the ipRGC and/or the rod signals.

Implementation of the method is advantageous when an experiment can be conducted with a spectrally tunable light source. Here, although the light source spectrum was not finely adjustable, the LED illumination has allowed us to create highly contrasting spectral power distributions that efficiently regulate receptor excitations in the short and middle wavelength range of the visible spectrum where receptor sensitivities are at a maximum. Indeed, we note that the spectral power distribution function of our illuminations resembles the example of frequency-limited functions representing spectral reflectance curves with a limited frequency of $\omega = 1/50$ [38].

B. ipRGC and/or Rod Response Isolation
Compared to other studies [37,39,40], it is a real advantage to be able to tune the stimulus with seven LEDs spanning the visible spectrum. It offers a nearly full spectrum illumination, which resembles an everyday light environment, in the laboratory. Also, it theoretically allows the experimenter to independently address up to seven photoreceptors. Regrettably, the higher the number of photoreceptor excitations to manipulate independently, the lower the achieved contrast. Here, as we allowed the ipRGC and rod to be excited at most or at least in parallel, only four photoreceptor systems were under control.

The rod contrast between the Mel Rod High and Mel Rod Low illuminations is equal to 1.44. This value is under the 80%
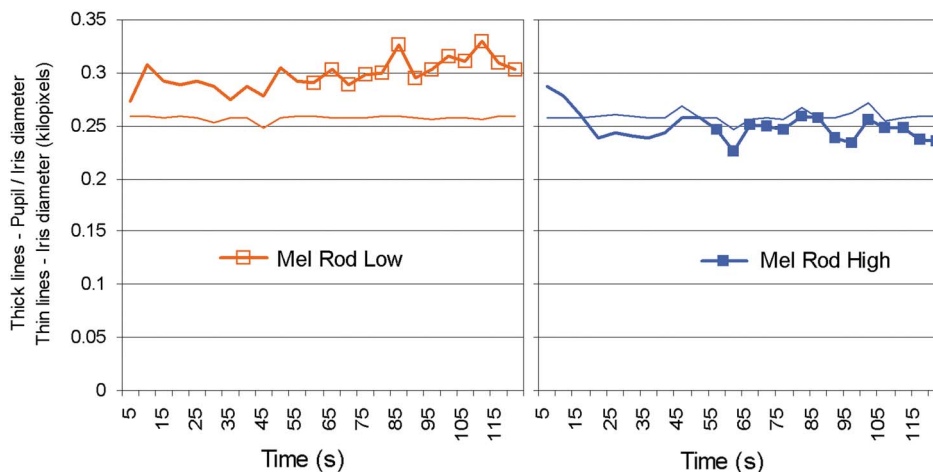

Fig. 8. (Color online) Ratio of pupil-to-iris diameter. Left panel: Measurements obtained under Mel Rod Low illumination. Right panel: Measurements obtained under Mel Rod High illumination. Symbols identify the measurements on which the average pupil-to-diameter ratio is calculated. Thin lines show the iris diameter in kilopixels. Example for observer #1.
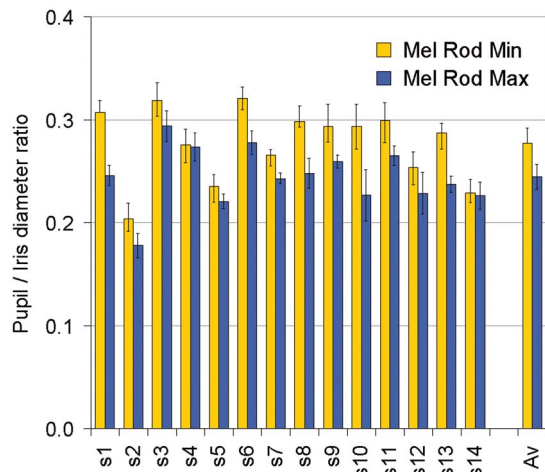
Fig. 9.   (Color online) Ratio and standard deviation of pupil-to-iris diameter measured in the melanopsin and rods minimum excitation condition and maximum excitation condition, for 14 observers, and average ratio.

rod modulation gamut provided by Cao et al. [40] for a desaturated orange or under the maximum symmetric 37% rod contrast calculated by Shapiro et al. [39] that yields 74% for the rod contrast gamut. Explanations might be found in the fact that the maximum obtainable contrast is dependent upon the number of receptors to control, the choice of primary stimuli, and the target chromaticity.

In a previous experiment [24], we had not succeeded in isolating the ipRGC response using silent substitution. No differential pupillary response could be observed with a variation of rod, ipRGC, or S-cone excitation alone. A differential pupillary response could only be obtained either by allowing for a joint variation of rods and ipRGCs or by silencing luminance instead of silencing M-cones and L-cones independently. In such cases, the ipRGC contrast was sufficiently high. [24]. As it is possible to achieve with seven LEDs an ipRGC contrast higher than with five LEDs, it would be valuable to attempt exclusive ipRGC isolation at our moderate photopic luminances.

Other strategies could be beneficial to isolate the contribution of the melanopsin expressing ipRGC response to pupillary light response. As the cones are responding transiently, and as the ipRGC response needs some time to establish, concentrating on the sustained pupil response is relevant. Nevertheless, rods as well as ipRGCs are eliciting a sustained response. To prevent the rod response, one possibility is to measure the pupil aperture during the cone plateau period, and the other is to operate at luminance levels that saturate the rod response. In the present study with seven LEDs, we used luminance levels that were favorable to isolate the melanopsin expressing ipRGC response. We actually ran the experiment at a scotopic luminance equal to 131 cd m^{-2} (Mel Rod Low) or 189 cd m^{-2} (Mel Rod High). Given the average pupil diameter equal to 5.3 and 4.6 mm, respectively, the scotopic troland value is about 3000 Td, close to rod saturation [39,41]. Although rods might have been active, melanopsin is probably the only photopigment operational after one minute of illumination under our experimental conditions.

C. Accuracy of the Experimental Metamers
We have already mentioned in the section "Illumination" that the far red color LED has been driven at a maximum intensity

in the Mel Rod High experimental configuration instead of the predicted intensity. This resulted in a minor increase of the L_{10} and the M_{10} excitation, which may have slightly contributed to the pupil constriction.

The primary goal of the experiment was to explore the domain of metamers that activate rods and ipRGCs differently and to accompany the reasoning with an experimental verification. On average, our experiments have shown that the replacement of the Mel Rod Low illumination by the Mel Rod High illumination elicits a significant pupil constriction. Nevertheless, several individual factors might influence the effect of light on an observer's ipRGC response.

On the one hand, we have not individually corrected the predicted spectra for individual variation of prereceptoral pigments. Lens absorption operates at short wavelength and affects the amount of light impacting all photoreceptors. Macular pigment, although concentrated in the foveal region, may affect the radiation reaching rods and cones.

On the other hand, the rationale of the experiment was to silence the three families of cones. In our experiment, we have supposed that the actual observer fundamentals conform to the ones recommended by the CIE [28]. And yet, the CIE report proposes an average of the cone fundamentals but has not given any consideration to interobserver variability [42,43,44]. Thus, it is likely that most of the 14 observers who took part in the experiment possess cone spectral sensitivities slightly different from the ones that have served in the computation of the cone silent illumination substitution. Indeed, the CIE 2006 fundamental approach [27,28] offers a way to estimate cone and rod responses once the macular pigment optical density and the lens optical density are individually estimated. The individual lens absorbance values could be used to profile individual cone, rod, and ipRGC responses [10,28].

Last, the pupil response and the pupil area vary from observer to observer. The pupil diameter decreases with age. For this reason, we have selected young observers, although how age affects ipRGCs function remains undetermined [11]. Further, besides illumination level and spectral light distribution, many parameters of the stimulus may alter the short-term or the long-term pupil response [45,46], and the ipRGC-controlled postillumination pupil response has a circadian rhythm independent of external light cues [47].

D. Application to Artificial Lighting
Metamerism is the basis of artificial lighting manufacturing. As it is costly to duplicate the spectrum of natural daylight, manufacturers only match the color of natural light. Thus, they produce artificial light that is metameric to natural light. Within the frame of black metamers, the difference between artificial light and natural light follows the difference between their black metamer component. Given the illuminants have identical color, they could have different effects on the visual nonimage response, in relation with the black metamer component.

LEDs are taking an increasing place in the domestic lighting market because they promise to produce light with low energy consumption. The white light emitted by the most common commercial LED is obtained by mixing the blue light emitted by a short wavelength diode and the yellow light emitted by fluorescence of a phosphor. The spectrum of the light emitted
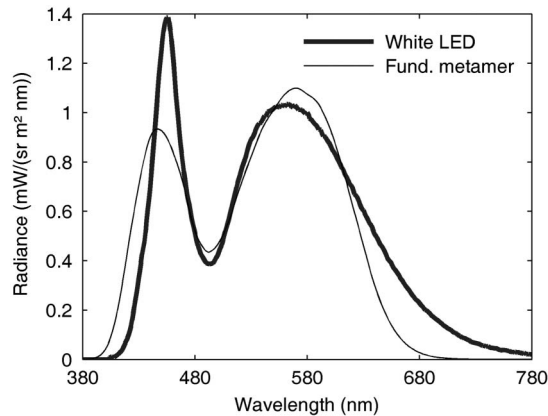
Fig. 10. Spectral radiance of a commercial white LED (thick line) and the fundamental metamer of natural daylight at 5350 K (thin line).

exhibits a narrow blue peak and a larger yellow peak. By controlling the deposit of fluorescent powder, the diode maker can adjust the color temperature.

It is more than a coincidence that the spectral light distribution of such a commercial LED is close to the fundamental metamer of natural daylight, as shown in Fig. 10. Even more, the balance between the narrow blue peak and the larger yellow peak, which is necessary to achieve a choice of color temperature, varies in parallel to the fundamental metamer spectrum. Therefore, two questions could be raised with respect to the use of the new LED technology.

First, what is special with the appearance of the white LED illumination? In the past, there have been many studies on the color rendition of light sources motivated by the fact that the CIE 1995 color rendering index R_a [48] fails to correspond to the perceived color quality of solid-state sources [49]. Today, several experimental investigations of the subjective appreciation of lighting color quality are being conducted, in terms of color fidelity, attractiveness, and naturalness [50,51]. Yet, a complete description of the color quality of a light source seems to be complex. Why does LED illumination look pleasant, whereas the color rendering is not appealing? Would a fundamental metamer illumination bring "color clarity" to surface colors and enhance the apparent contrast between them?

Second, could the presence or the absence of black metamers within artificial light have an effect on visual performance and visual comfort? Is the effect of black metamers on the nonimaging responses the only consequence of a particular spectral design? What about visual performance, visual comfort, glare? Any deficit of pupil constriction owing to a radiation similar to the fundamental metamer such as the LED radiation would not be favorable to glare limitation [11]. There is some concern about light directly emitted by high correlated color temperature LEDs [52,53]. In a LED, the chip that emits light is so small that, although the flux emitted may be moderate, the luminance may be extremely high. If pupillary reflex could decrease owing to the very low 480 nm light emission, retinal exposure to blue light hazard might be increased [53].

6. CONCLUSION

Black metamers are appropriate stimuli to explore the excitation of photoreceptors besides cones. We have explored the theoretical limits of the domain of white metamers that excite

ipRGCs and/or rods. We have used a seven-color LED illumination system to implement a black metamer approach and study rod and ipRGC responses. Monitoring multicolor LED illumination, we have verified for all observers that varying the ipRGC and rod excitations simultaneously modifies the relative sustained pupil diameter by 12%. We question the possible impairment of performance and visual comfort of any unnatural pupil aperture that could result from artificial light designs.

REFERENCES

1. D. M. Berson, F. A. Dunn, and M. Takao, "Phototransduction by retinal ganglion cells that set the circadian clock," Science **295**, 1070–1073 (2002).
2. S. Hattar, H. W. Liao, M. Takao, D. M. Berson, and K. W. Yau, "Melanopsin-containing retinal ganglion cells: architecture, projections, and intrinsic photosensitivity," Science **295**, 1065–1070 (2002).
3. D. M. Dacey, H.-W. Liao, B. B. Peterson, F. R. Robinson, V. C. Smith, J. Pokorny, K.-W. Yau, and P. D. Gamlin, "Melanopsin-expressing ganglion cells in primate retina signal colour and irradiance and project to the LGN," Nature **433**, 749–754 (2005).
4. P. R. Jusuf, S. C. Lee, J. Hannibal, and U. Grünert, "Characterization and synaptic connectivity of ipRGC-containing ganglion cells in the primate retina," Eur. J. Neurosci. **26**, 2906–2921 (2007).
5. M. T. Hoang Do and K.-W. Yau, "Intrinsically Photosensitive Retinal Ganglion Cells," Physiol. Rev. **90**, 1547–1581 (2010).
6. K. Y. Wong, F. A. Dunn, and D. M. Berson, "Photoreceptor adaptation in intrinsically photosensitive retinal ganglion cells," Neuron **48**, 1001–1010 (2005).
7. T. M. Schmidt and P. Kofuji, "Functional and morphological differences among intrinsically photosensitive retinal ganglion cells," J. Neurosci. **29**, 476–482 (2009).
8. D. C. Tu, D. Zhang, J. Demas, E. B. Slutsky, I. Provencio, T. E. Holy, and R. N. Van Gelder, "Physiologic diversity and development of intrinsically photosensitive retinal ganglion cells," Neuron **48**, 987–999 (2005).
9. R. J. Lucas, S. Hattar, M. Takao, D. M. Berson, R. G. Foster, and K. W. Yau, "Diminished pupillary light reflex at high irradiances in melanopsin-knockout mice," Science **299**, 245–247 (2003).
10. P. D. R. Gamlin, D. H. McDougal, J. Pokorny, V. C. Smith, K. W. Yau, and D. M. Dacey, "Human and macaque pupil responses driven by melanopsin-containing retinal ganglion cells," Vis. Res. **47**, 946–954 (2007).
11. E. L. Markwell, B. Feigl, and A. J. Zele, "Intrinsically photosensitive melanopsin retinal ganglion cell contributions to the pupillary light reflex and circadian rhythm," Clin. Exp. Optom. **93**, 137–149 (2010).
12. Y. Fu, H. Zhong, M.-H. H. Wang, D.-G. Luo, H.-W. Liao, H. Maeda, S. Hattar, L. J. Frishman, and K.-W. Yau, "Intrinsically photosensitive retinal ganglion cells detect light with a vitamin A-based photopigment, ipRGC," Proc. Natl. Acad. Sci. USA **102**, 10339–10344 (2005).
13. L. S. Mure, P.-L. Cornut, C. Rieux, E. Drouyer, P. Denis, C. Gronfier, and H. M. Cooper, "Melanopsin bistability: a fly's eye technology in the human retina," PLoS ONE **4**(6), e5991, 1–10 (2009), www.plosone.org.
14. S. Panda, S. K. Nayak, B. Campo, J. R. Walker, J. B. Hogenesch, and T. Jegla, "Illumination of the IpRGC signaling pathway," Science **307**, 600–604 (2005).
15. M. W. Hankins, S. N. Peirson, and R. G. Foster, "Melanopsin: an exciting photopigment," Trends Neurosci. **31**, 27–36 (2008).

16. K. Mawad and R. N. Van Gelder, "Absence of longwavelength photic potentiation of murine intrinsically photosensitive retinal ganglion cell firing in vitro," J. Biol. Rhythms **23**, 387–391 (2008).

17. D. H. McDougal and P. D. Gamlin, "The influence of intrinsically-photosensitive retinal ganglion cells on the spectral sensitivity and response dynamics of the human pupillary light reflex," Vis. Res. **50**, 72–87 (2010).

18. M. Alpern and F. W. Campbell, "The behaviour of the pupil during dark-adaptation," J. Physiol. **165** (Suppl), 5P–7P (1963).

19. L. Kankipati, C. A. Girkin, and P. D. Gamlin, "Post-illumination Pupil Response in Subjects without Ocular Disease," Investig. Ophthalmol. Vis. Sci. **51**, 2764–2769 (2010).

20. R. S. L. Young and E. Kimura, "Pupillary correlates of light-evoked melanopsin activity in humans," Vis. Res. **48**, 862–871 (2008).

21. D. H. Sliney, "From photobiological science to lighting applications," in Proceedings of the 2nd CIE Expert Symposium on Lighting and Health, CIE x031:2006 (2006), pp. 1–5.

22. G. C. Brainard, D. Sliney, J. P. Hanifin, G. Glickman, B. Byrne, J. M. Greeson, S. Jasser, E. Gerner, and M. D. Rollag, "Sensitivity of the human circadian system to short-wavelength (420-nm) light," J. Biol. Rhythms **23**, 379–386 (2008).

23. S. Tsujimura, K. Ukai, D. Ohama, A. Nuruki, and K. Yunokuchi, "Contribution of human melanopsin retinal ganglion cells to steady-state pupil responses," Proc. R. Soc. B **277**(1693), 2485–2492 (2010).

24. F. Viénot, S. Bailacq, and J. Le Rohellec, "The effect of controlled photopigment excitations on pupil aperture," Ophthal. Physiol. Opt. **30**, 484–491 (2010).

25. G. Wyszecki, "Evaluation of metameric colors," J. Opt. Soc. Am. **48**, 451–452 (1958).

26. J. B. Cohen and W. E. Kappauf, "Metameric color stimuli, fundamental metamers, and Wyszecki's metameric blacks," Am. J. Psychol. **95**, 537–564 (1982).

27. A. Stockman and L. T. Sharpe, "Cone spectral sensitivities and color matching," in *Color Vision: From Genes to Perception*, K. R. Gegenfurtner and L. T. Sharpe, eds. (Cambridge University Press, 2000), pp. 53–87, http://www.cvrl.org.

28. CIE, "Fundamental chromaticity diagram with physiological axes—part 1," CIE Publ.170-1:2006 (CIE, 2006).

29. CIE, "International electrotechnical vocabulary," CIE Publ. 17.4 (CIE, 1987), 845-01-22, http://www.electropedia.org/iev/iev.nsf/index?openform&part=845.

30. M. T. H. Do, S. H. Kang, T. Xue, H. Zhong, H.-W. Liao, D. E. Bergles, and K.-W. Yau, "Photon capture and signalling by melanopsin retinal ganglion cells," Nature **457**, 281–288 (2009).

31. J. al Enezi, V. Revell, T. Brown, J. Wynne, L. Schlangen, and R. Lucas, "A 'melanopic' spectral efficiency function predicts the sensitivity of IpRGC photoreceptors to polychromatic lights," J. Biol. Rhythms **26**, 314–323 (2011).

32. J. D. Bullough, M. G. Figueiro, B. P. Possidente, R. H. Parsons, and M. S. Rea, "Additivity in Murine Circadian Phototransduction," Zool. Sci. **22**, 223–227 (2005).

33. Colorimetry tables were downloaded at http://www.cvrl.org.

34. L. T. Sharpe, A. Stockman, W. Jagla, and H. Jägle, "A luminous efficiency function, $V^*_{D65}(\lambda)$, for daylight adaptation: a correction," Color Res. Appl. **36**, 42–46 (2011).

35. Y. Le Grand, *Light, Color and Vision*, 2nd ed. (Chapman and Hall, 1968), p. 86, Eq. 59.

36. D. van Norren and J. J. Vos, "Spectral transmission of the human ocular media," Vis. Res. **14**, 1237–1244 (1974).

37. O. Estevez and H. Spekreijse, "The 'silent substitution' method in visual research," Vis. Res. **22**, 681–691 (1982).

38. W. S. Stiles, G. Wyszecki, and N. Ohta, "Counting metameric object-color stimuli using frequency-limited spectral reflectance functions," J. Opt. Soc. Am. **67**, 779–784 (1977).

39. A. G. Shapiro, J. Pokorny, and V. C. Smith, "Cone-rod receptor spaces with illustrations that use CRT phosphor and light-emitting-diode spectra," J. Opt. Soc. Am. A **13**, 2319–2328 (1996).

40. D. Cao, J. Pokorny, V. C. Smith, and A. J. Zele, "Rod contributions to color perception: Linear with rod contrast," Vis. Res. **48**, 2586–2592 (2008).

41. M. Aguilar and W. S. Stiles, "Saturation of the rod mechanism of the retina at high levels of stimulation," Opt. Acta **1**, 59–65 (1954).

42. W. S. Stiles and J. M. Burch, "N.P.L. colour-matching investigation: final report," Opt. Acta **6**, 1–26 (1959).

43. A. Stockman, D. I. A. MacLeod, and N. E. Johnson, "Spectral sensitivities of human cones," J. Opt. Soc. Am. A **10**, 2491–2521 (1993).

44. A. Sarkar, F. Autrusseau, F. Viénot, P. Le Callet, and L. Blondé, "From CIE 2006 physiological model to improved age-dependent and average colorimetric observers," J. Opt. Soc. Am. A **28**, 2033–2048 (2011).

45. J. L. Barbur, "Learning from the pupil—studies of basic mechanisms and clinical applications," in *The Visual Neurosciences*, L. M. Chalupa and J. S. Werner, eds. (MIT Press, 2004), Vol. **1**, pp. 641–656.

46. W. Bi and J. L. Barbur, "Revisiting pupil colour responses," presented at the 21st Symposium of the International Colour Vision Society, Kongsberg, Norway, 1–5 July 2011.

47. A. J. Zele, B. Feigl, S. S. Smith, and E. L. Markwell, "The circadian response of intrinsically photosensitive retinal ganglion cells," PLoS ONE **6**(3), doi: 10.1371/journal.pone.0017860, e17860 (2011).

48. CIE, "Method of measuring and specifying color rendering properties of light sources, CIE Publ. 13.2 (CIE, 1995).

49. W. Davis and Y. Ohno, "Towards an improved color rendering metric," Proc. SPIE **5941**, 1G1–8 (2005).

50. R. Smet, W. R. Ryckaert, M. R. Pointer, G. Deconinck, and P. Hanselaer, "Correlation between color quality metric predictions and visual appreciation of light sources," Opt. Express **19**, 8151–8166 (2011).

51. S. Boissard-Jost and M. Fontoynont, "Optimization of LED-based light blendings for object presentation," Color Res. Appl. **34**, 310–320 (2009).

52. ANSES, "Health effects of lighting systems using light-emitting diodes (LEDs)," opinion of the French agency for food, environmental and occupational health and safety in response to the internally solicited request (ANSES, 2010).

53. F. Behar-Cohen, C. Martinsons, F. Viénot, G. Zissis, A. Barlier-Salsi, J. P. Cesarini, O. Enouf, M. Garcia, S. Picaud, and D. Attia, "Light-emitting diodes (LED) for domestic lighting: Any risks for the eye?" Prog. Retin. Eye Res. **30**, 239–257 (2011).